Near-field blast vibration models

Dane Blair and Alan Minchinton
Orica Australia

ABSTRACT

There is a persistent use of the Holmberg-Persson near-field vibration damage model despite the fact that ten years ago it was shown to be incorrect on the grounds of simple physics. In order to address this problem, the detailed recipe for a new, easily implemented model is presented. This new model, the Scaled Heelan model, is based on a standard Heelan (waveform) model altered to incorporate charge weight scaling. This Scaled Heelan model, thus, maintains some aspects of the original spirit of the Holmberg-Persson approach. A comparison of the Heelan models, a dynamic finite element model (DFEM) and a new full-field model is given, showing good agreement between the DFEM and full-field solutions in all cases. However, the Heelan models show some discrepancies for certain frequencies of wave propagation, even at large distances from the source. Nevertheless, these Heelan models have value simply because they include influences such as the detonation velocity and the various wave types, and, furthermore, require significantly less computing time than that required for either the DFEM or full-field solutions.

INTRODUCTION

Holmberg and Persson (1979) developed a near-field vibration model in which the standard charge weight scaling law was used to estimate the peak vibration level due to a blasthole explosive source. In this model, the continuous length of explosive was modelled by summing charge elements along the borehole. However, Blair and Minchinton (1996) showed that this model was unsound because it did not correctly sum (integrate) the vibration contribution from each charge element. This unfortunate situation arose because the charge weight scaling law does not contain waveform information and hence cannot provide any rational means of estimating the total peak vibration level from the sum of waveforms that would be produced by all elements of a charge.

However, despite this apparently well-known and fatal flaw, the Holmberg-Persson model still remains popular within the blast research community (see for example, Adamson and Scherpenisse, 1998; Liu et al, 1998; McKenzie, 1999; Keller and Kramer, 2000; Ryan and Harris, 2000; Keller and Ryan, 2001; Hustrulid and Wenbo, 2002; McKenzie and Holley, 2004; Onderra and Esen, 2004; Onderra, 2004; Villaescusa et al, 2004). We find this stance difficult to understand. It may be due, in part, to misconceptions with regard to waveform superposition and aspects of rock dynamics. For example, to paraphrase Villaescusa et al (2004), the Holmberg-Persson technique models blast wave attenuation but it is essentially a time independent (static) approach. These same workers then admit that the technique produces results that are incompatible with (realistic) dynamic models, yet go on, quite confusingly, to

claim that the results, nevertheless, are practical and useful. Clearly, this viewpoint makes little sense. Furthermore, if any model has a demonstrated fatal flaw then it must be discarded, irrespective of whether or not it happens to agree with experiment – to do otherwise is against a basic tenet of science.

Support for the Holmberg-Persson model appears to be deep-rooted, and the findings of Blair and Minchinton (1996) are either unknown, ignored or misconstrued. As an example, Hustrulid and Wenbo (2002) incorrectly stated that 'Blair and Minchinton (1996) even pointed out that the Holmberg-Persson model *might* be theoretically in error'. In fact Blair and Minchinton demonstrated, quite clearly and using simple physics, that this model *was* in error. Furthermore, Hustrulid and Wenbo (2002) then attempt to justify their particular model by claiming that it gave results similar to the Holmberg-Persson predictions. Thus on one hand they appear to admit the possibility that this model might be incorrect, yet on the other hand seem content to use it as a yardstick to judge the validity of their own model.

The Holmberg-Persson model is invalid in the near-field, and in the far-field it simply collapses to the standard charge weight scaling law (Blair and Minchinton, 1996). Thus there is no reason to ever require the model. In view of this situation, a main aim of the present work is to document the Heelan waveform vibration model, the results of which were originally reported in Blair and Minchinton (1996). However, since many researchers and practitioners remain comfortable with charge weight scaling laws, this model is altered to ensure that each elemental Heelan waveform has a peak particle velocity given by a simple scaling law. In this regard at least, there is some aspect of commonality between the Scaled Heelan and the Holmberg-Persson models. The vector peak particle velocity, *vppv*, due to the entire length of charge is then obtained by an appropriate superposition of all elemental Scaled Heelan waveforms. The Scaled Heelan model as well as the original Heelan model discussed in Blair and Minchinton (1996) have been developed by one of us (DB).

It should be appreciated that, under its basic assumptions, the general solution derived by Heelan (1953) for the particle displacement due to a pressurised cylindrical element is physically and mathematically well founded (Meredith, 1990). However, Blair (2005) has used a full-field solution to this problem and found that the Heelan solution is a valid approximation at large distances only for certain vibration frequencies produced by the charge. Thus another main aim of the present work is to give the near-field vibration predictions of the Heelan and full-field solutions for a blasthole of specified length and explosive velocity of detonation and then to compare these results with a dynamic finite element model (DFEM) of the blasthole vibration. The vibration attribute of present interest is the particle velocity rather than the particle displacement.

THE HEELAN MODEL

Models are now presented (in recipe form) that use full waveform superposition in order to predict the total horizontal, $v_r(r,z,t)$, and vertical, $v_z(r,z,t)$, components of the particle velocity at any monitoring point, P(r,z), due to an explosive column of length L in a hole of infinite length embedded in a medium of infinite extent. The geometry is illustrated in Figure 1, which shows five representative elements including the first

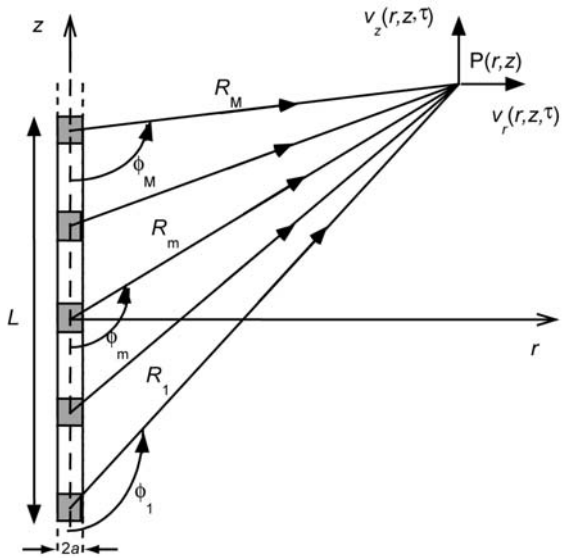

Fig 1 - The blasthole geometry

and last (*M*th) elements as well as a general (*m*th) element. The full waveform solution at P is obtained by summing the waveform contributions from all *M* elements, each having a length δL (= *L*/*M*).

In all the models to be discussed the blasthole pressure-time function applied to each element is assumed to have the form:

$$P(t) = H(t)P_o t^n e^{-bt} \tag{1}$$

where *t* is time, *n* and *b* are constants, P_o is a suitable normalising factor and $H(t)$ is the Heaviside step function given by $H(t) = 0$ if $t \le 0$, $H(t) = 1$ if $t > 0$. The standard Heelan model is considered first, and then it is altered to produce a scaled version based on a charge weight scaling law.

If a general dimensionless time variable is defined as $\tau = bt$, then a (dimensionless) time associated with the *m*th explosive element can be defined by

$\tau_m = \tau - b(m-1)\delta L/V_D$, where V_D is the explosive velocity of detonation. In this notation, the waveform superposition equations describing the total radiation from all *M* charge elements are:

$$v_r(\tau) = \sum_{m=1}^{M}[v_{Rm}(\tau_m)\sin\phi_m + v_{\phi m}(\tau_m)\cos\phi_m] \tag{2}$$

$$v_z(\tau) = \sum_{m=1}^{M}[-v_{Rm}(\tau_m)\cos\phi_m + v_{\phi m}(\tau_m)\sin\phi_m] \tag{3}$$

where R_m and ϕ_m are shown in Figure 1, along with the velocity components $v_r(\tau)$ and $v_z(\tau)$, where the *r,z* dependence has been dropped for convenience. Furthermore, if *a* is the radius of the blasthole, and α and β are the P-wave and S-wave velocities, respectively, then the *R* and ϕ components for each element are given by the Heelan solution to the pressure load $P(\tau)$:

$$v_{Rm}(\tau) = \frac{C}{R_m}H(\tau_{pm})(\tau_{pm}^n - 2n\tau_{pm}^{n-1} + n(n-1)\tau_{pm}^{n-2})(1 - 2\frac{\beta^2}{\alpha^2}\cos^2\phi_m)e^{-\tau_{pm}} \tag{4}$$

and

$$v_{\phi m}(\tau) = \frac{C}{R_m}H(\tau_{sm})(\tau_{sm}^n - 2n\tau_{sm}^{n-1} + n(n-1)\tau_{sm}^{n-2})(\frac{\alpha}{\beta}\sin 2\phi_m)e^{-\tau_{sm}} \tag{5}$$

where C is a constant for any one model and is given by:

$$C = \frac{w_e b^{2-n} P_o}{2\pi\rho_e \mu\alpha} \qquad (6)$$

where μ is the rock shear modulus, $w_e = \pi\rho_e a^2 \delta L$ and is the (constant) mass of each charge element and ρ_e its (explosive) density. Furthermore, $\tau_{pm} = \tau_m - bR_m/\alpha$ and $\tau_{sm} = \tau_m - bR_m/\beta$ and are the total dimensionless P- and S-wave traveltimes, respectively, that also include the element delay initiation times. As before, $H(\tau_{pm}) = 0$ if $\tau_{pm} \leq 0$ and $H(\tau_{pm}) = 1$ if $\tau_{pm} > 0$; $H(\tau_{sm})$ is similarly defined. The vector waveform is then given by:

$$V(\tau) = \sqrt{v_r^2(\tau) + v_z^2(\tau)} \qquad (7)$$

Equations (1) to (7) completely describe the Heelan solution for the particle velocity recorded at any monitoring site. It is a simple matter to calculate the vector peak particle velocity (*vppv*), which is the maximum value of $V(\tau)$ over all τ. The results shown in Blair and Minchinton (1996) were obtained using the following parameters: $n = 6$, $b = 10\,000$, $L = 5$ m, $a = 0.1$ m,
$\alpha = 5500$ m/s and $\beta = 3175$ m/s. The solution was found to satisfactorily converge for $M = 41$ elements in the blasthole. The parameter P_o of equation (1) was set at 1.0 because only normalised contours of velocity were investigated.

A SCALED HEELAN MODEL

It should be appreciated that it is very difficult to estimate a realistic numerical value for the parameter P_o of equation (1) because there is currently little understanding of the effective vibrational load of an explosive at the blasthole walls. It was for this reason that P_o was set at 1.0 in the Heelan model of equations (4) to (6) which can only be used to predict normalised vibration values. This model is now altered in order to predict absolute values of vibration that are governed by the experimentally determined parameters of charge weight scaling laws which are independent of P_o.

So far the vector peak particle velocity, *vppv*, due to the summation of all M elements, has been determined without any need to consider the vector peak particle velocity, $vppv_m$, say, of any individual (mth) element. However, it should also be appreciated that given only the values of all the $vppv_m$ there is no rational method that can be used to predict *vppv* because wave superposition and vector summation are required (equations 2, 3 and 7). Unfortunately, since the Holmberg-Persson model is not based on waveforms, it attempts to use only the $vppv_m$ to predict *vppv*, and this is the essence of its fatal flaw. Nevertheless, within the spirit of the Holmberg-Persson approach, it is worthwhile investigating a waveform model in which each elemental waveform has a peak vibration given by charge weight scaling. Thus the basic assumption of this model is:

$$vppv_m = K w_e^A R_m^{-B} \qquad (8)$$

where K, A and B are the usual site constants. However, such an assumption raises four immediate problems. Firstly, the Heelan model requires that the peak vibration from the general (mth) single element decays as R_m^{-1} and not R_m^{-B} (equations 4, 5). Secondly, this peak vibration is also proportional to w_e and not w_e^A (equation 6). Thirdly, the Heelan model depends on the angle ϕ_m, whereas the charge weight scaling law is independent of this

angle. Fourthly, the charge weight scaling law (8) is dimensionally unsound. All these problems are now discussed.

If $B > 1.0$, then there is a possible remedy for the first problem by acknowledging that material attenuation (which is not included in the Heelan solution) requires waveform attenuation at a rate greater than R_m^{-1}. Since $R_m^{-B} = R_m^{-1} R_m^{-(B-1)}$, then it is reasonable to view the extra attenuation, $R_m^{-(B-1)}$, as being due to material attenuation inherent to the scaling laws which are based on experimental observations. In this case, the parameter R_m^{-1} in equations (4) and (5) could simply be replaced by R_m^{-B}. If the site parameter B is found to be less than 1.0 in a given experimental investigation, then it is clear that the charge weight scaling law applied to the particular data is in direct conflict with fundamental theories of wave propagation from blastholes. In this regard it is worthwhile noting that Holmberg and Persson (1979) suggest that $B = 1.5$ can be used as a standard value.

The second problem can be addressed using an appropriate normalisation to ensure that the peak particle velocity for an element is proportional to $w_e^A R_m^{-B}$. For example, if γ_n is a constant dependent only on n, then the waveforms of equations (4) and (5) are governed by a (normalised and dimensionless) wave shape, $s(\tau)$, which has a maximum value of unity:

$$s(\tau) = \gamma_n (\tau^n - 2n\tau^{n-1} + n(n-1)\tau^{n-2}) e^{-\tau} \tag{9}$$

A numerical evaluation of (9) yields $\gamma_n = 0.9910$ for $n = 3$ and $\gamma_n = 0.0455$ for $n = 6$. Thus if the parameter C/R_m (equations 4, 5, 6) is replaced by $\gamma_n K w_e^A R^{-B}$, then each elemental waveform, for $\phi_m = \pi/2$ at least, will have a vector peak particle velocity given by the charge weight scaling law of equation (8).

The third problem arises when $\phi_m \neq \pi/2$. In this case there can be no rationalisation between charge weight scaling concepts and the traditional Heelan solution, and so there is no option but to retain the $cos^2\phi_m$ and $sin2\phi_m$ terms of equations (4) and (5). After all, these terms do describe the radiation patterns of P- and S-waves and so are important for any realistic vibration wave model. Thus, in summary, the Scaled Heelan model is defined by replacing the elemental waveforms of equations (4) and (5) by:

$$v_{Rm}(\tau) = \frac{\gamma_n K w_e^A}{R_m^B} H(\tau_{pm})(\tau_{pm}^n - 2n\tau_{pm}^{n-1} + n(n-1)\tau_{pm}^{n-2})(1 - 2\frac{\beta^2}{\alpha^2}\cos^2\phi_m) e^{-\tau_{pm}} \tag{10}$$

and

$$v_{\phi m}(\tau) = \frac{\gamma_n K w_e^A}{R_m^B} H(\tau_{sm})(\tau_{sm}^n - 2n\tau_{sm}^{n-1} + n(n-1)\tau_{sm}^{n-2})(\frac{\alpha}{\beta}\sin 2\phi_m) e^{-\tau_{sm}} \tag{11}$$

This model is independent of P_o and can be used to calculate absolute levels of vibration (or peak vibration) based on site constants, K, A and B, obtained from appropriate charge weight scaling laws. Strictly speaking, any experimental determination of the site constants for each element should be obtained only when $\phi_m = \pi/2$ which may sometimes be impractical.

With regard to the fourth problem, it should be appreciated that the standard Heelan solution is dimensionally sound because it is based on accepted elastic wave theory.

Indeed, C/R_m is the only non-dimensionless parameter in equations (4) and (5) describing the velocity components $v_{Rm}(\tau)$ and $v_{\phi m}(\tau)$. From equation (1) it is clear that P_o has dimensions of a pressure multiplied by time^{-n}. Furthermore, since μ has the dimension of pressure, and b has the dimension of inverse time, then C of equation (6) has dimensions of length^2/time and thus C/R_m has the required dimensions of velocity. However, the Scaled Heelan solution is not dimensionally sound because the parameter $w_e^A R_m^{-B}$ in equations (10) and (11) will continually change its dimensions depending on the experimental values determined for A and B. Blair (2004) has discussed the dimensionally unsound nature of charge weight scaling laws, and this is yet another example. Unfortunately, there is no remedy for this problem, which also plagues most blast vibration models including the Holmberg-Persson model. Perhaps the best way to view the Scaled Heelan model is that it does, at least, use full waveform superposition to provide numerical values for the particle velocity at each instant in time.

MODEL COMPARISONS

All the following models use the parameter values set by Blair and Minchinton (1996), unless stated otherwise; these particular values have been listed above. It should also be noted here that we subsequently found an error in our previous DFEM results, but only for the case of the 5 m column of charge with a finite velocity of detonation (5500 m/s). This error has now been corrected.

There are four distinct models considered here – the Heelan, the Scaled Heelan, the full-field and DFEM. The solutions are presented as contour levels of *vppv* surrounding the particular charge in the blasthole. With the exception of the Scaled Heelan model, all contour levels are normalised to unity at the point 5 m horizontally out from the centre of the charge length, and given for the range 0.2 to 2.0 in increments of 0.2. For the Scaled Heelan model, the suggested values of Holmberg and Persson (1979) are used for the site constants of equation (8), and are K = 700, A = 0.7 and B = 1.5. The contour levels shown for this model are in units of mm/s surrounding the charge. Solutions for a single charge element of length 0.2 m centred at (0,0) are presented first, followed by solutions for an extended column of explosive of length 5 m, centred at (0,0), base-primed and having a velocity of detonation of 5500 m/s.

Single element of charge

Figure 2 shows the Heelan predictions for the contours of normalised *vppv* surrounding a cylindrical element and Figure 3 shows the Scaled Heelan predictions for the absolute values of *vppv* (in mm/s). In the Scaled Heelan model, the mass, w_e, of the element is 5.21 kg and is based on an ANFO explosive having ρ_e = 830 kg/m^3. Thus for a distance of 5 m, the charge weight scaling law (equation 8) directly yields a $vppv_m$ of approximately 200 mm/s.

Figure 3 shows this peak value at a location 5 m along the horizontal direction through the centre of the charge for which $\phi = \pi/2$, where only P-waves propagate. For other locations the motion is markedly different due to the presence of S-waves as well as P-waves. In fact for locations given by $\phi = \pm\pi/4$ and $\phi = \pm 3\pi/4$, the charge weight scaling law significantly underestimates the true vibration which is dominated by the shear-vertical (SV) wave – this wave type can promote a high degree of damage around any blasthole.

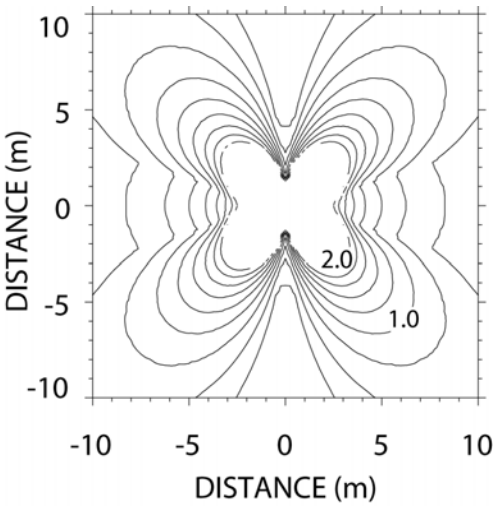

Fig 2 - The Heelan predictions for normalised *vppv* from a single element of charge

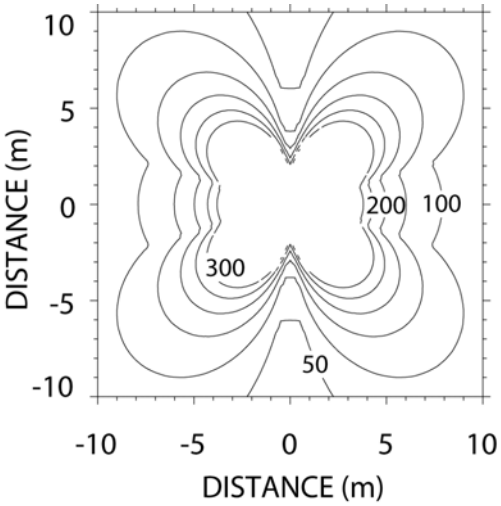

Fig 3 - The Scaled Heelan predictions for *vppv* (mm/s) from a single element of charge

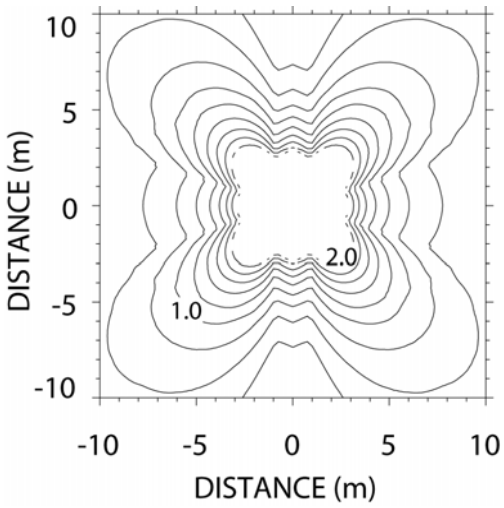

Fig 4 - The full-field predictions for normalised *vppv* from a single element of charge

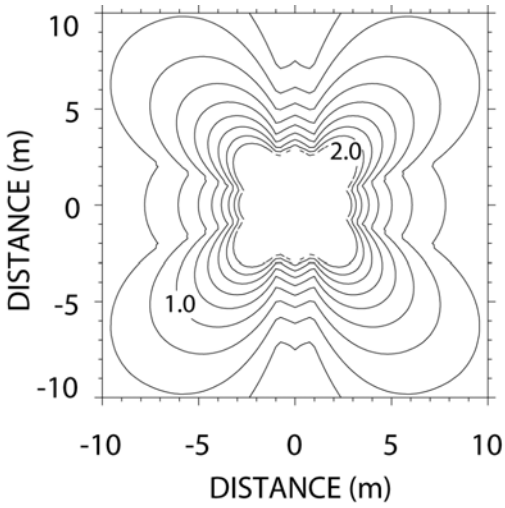

Fig 5 - The DFEM predictions for normalised *vppv* from a single element of charge

Figure 4 shows the normalised *vppv* for the full-field solution – the details of this model have been given in Blair (2005) and will not be repeated here. Figure 5 shows the DFEM results. There is good agreement between the *vppv* predictions of these models and Blair (2005) shows that there is also good agreement between the waveform shapes as well.

Comparing figures 2 and 3 with figures 4 and 5, clearly shows that the Heelan solutions underestimate the vibration near the blasthole wall (ϕ close to 0 or π) for which the S-wave motion is approaching zero (equation 11). However, in reality, S-waves will propagate along the blasthole wall and into nearby regions, and such motion is correctly predicted by the full-field and DFEM solutions. Due to the difficult nature of the full-field solution, Blair (2005) was unable to find a simplified expression for the motion near the wall. Nevertheless, this analysis did provide further (confidential) insights and these have been used to improve the Scaled Heelan solution in this region.

A column of explosive

Figure 6 shows the Heelan predictions for the contours of normalised *vppv* surrounding a 5m column of charge and Figure 7 shows the absolute values of *vppv* (in mm/s) predicted by the improved version of the Scaled Heelan model.

Figure 8 shows the normalised *vppv* for the full-field solution and Figure 9 shows the DFEM results. Although the full-field model and the DFEM are vastly different approaches, they both account for the (elastic) motion at all frequencies and for all regions surrounding the blasthole. Again, the predictions of these models are seen to be in good agreement.

The solutions presented so far have been obtained for parameter values $n = 6$ and $b = 10\ 000$. These parameters determine the frequency content of the applied pressure function, $P(t)$, of equation (1), and hence determine the frequency content of the radiated blast vibration waves. In this regard, Blair (2005) proved that for n = 6 the average frequency of the vibration waves is given by $f_A = 0.0597b$. Thus for b=10 000 the average frequency of the radiated waves is 597 Hz. In some of our open pit and underground blast damage investigations we have observed typical values of f_A between 200 Hz and 3000 Hz (or higher); these two mean frequencies correspond to $b = 3350$ and $b = 50250$, respectively.

Figures 10 and 11 show the Heelan and full-field results for relatively low-frequency waves given by $b = 3000$; Figures 12 and 13 show the Heelan and full-field results for high-frequency waves given by $b = 50\ 000$. It is obvious that there are increased discrepancies in the radiation patterns between both models for both high and low frequencies. All contour levels have been normalised to the location (5,0), and so give no information on absolute levels of vibration. However, Blair (2005) shows that in the low frequency regime, the Heelan solution overestimates the true vibration (as given by the full-field solution) and in the

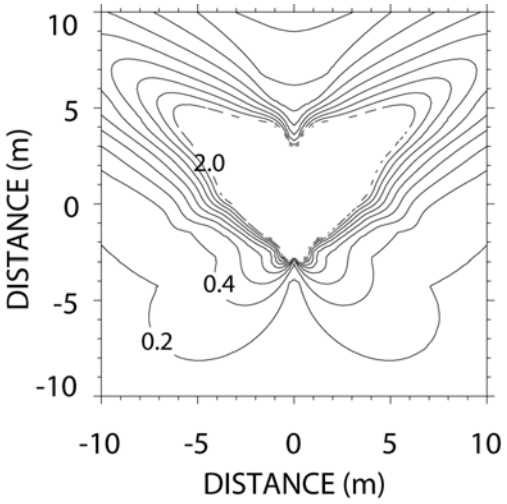

Fig 6 - The Heelan predictions for normalised *vppv* from a 5 m column of charge

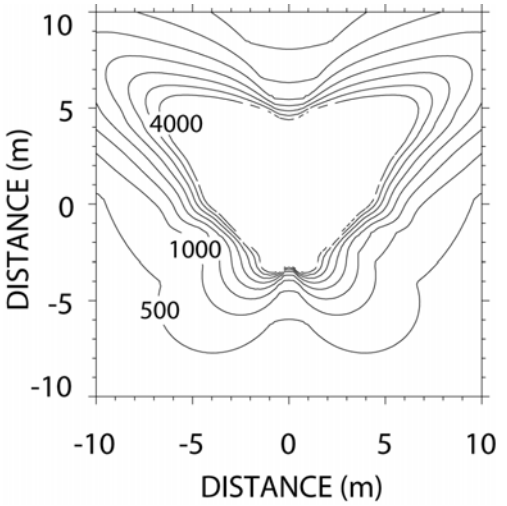

Fig 7 - The Scaled Heelan predictions for *vppv* (mm/s) from a 5 m column of charge

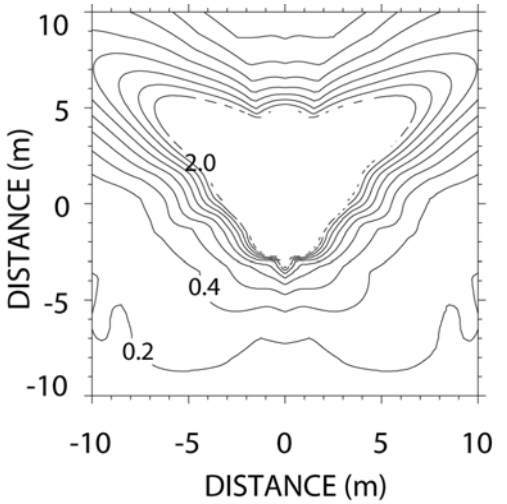

Fig 8 - The full-field predictions for normalised *vppv* from a 5 m column of charge

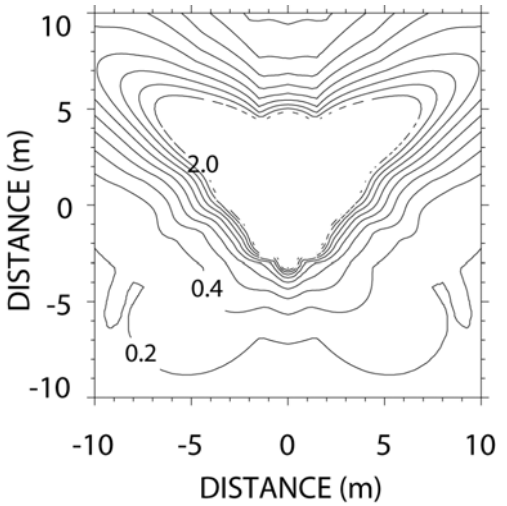

Fig 9 - The DFEM predictions for normalised *vppv* from a 5 m column of charge

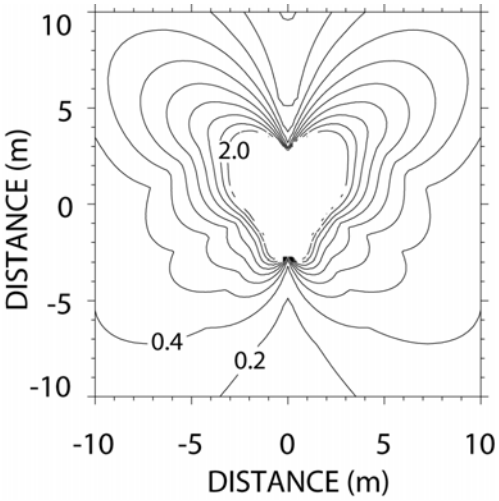

Fig 10 - The Heelan predictions for b = 3000 (f_A = 179 Hz) (5 m column of charge)

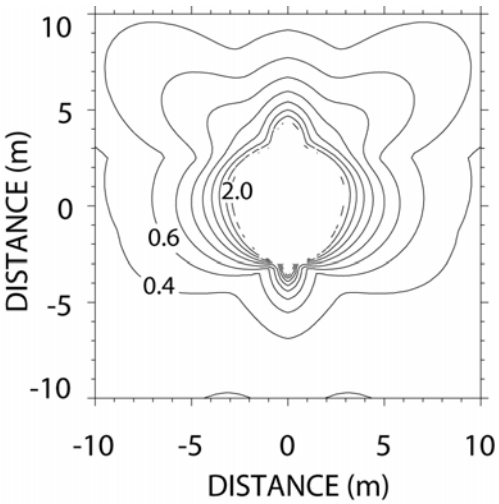

Fig 11 - The full-field predictions for b = 3000 (f_A = 179 Hz) (5 m column of charge)

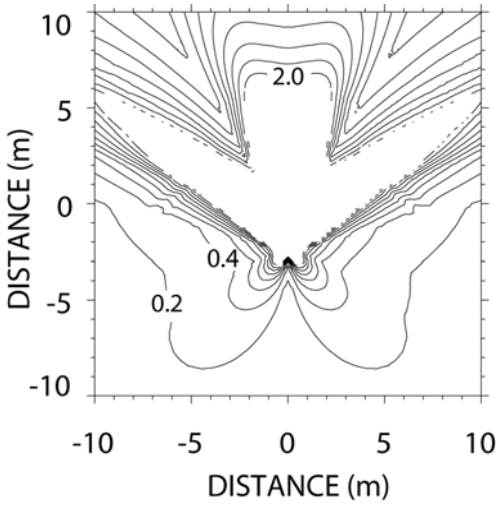

Fig 12 - The Heelan predictions for b = 50 000, (f_A = 2985 Hz) (5 m column of charge)

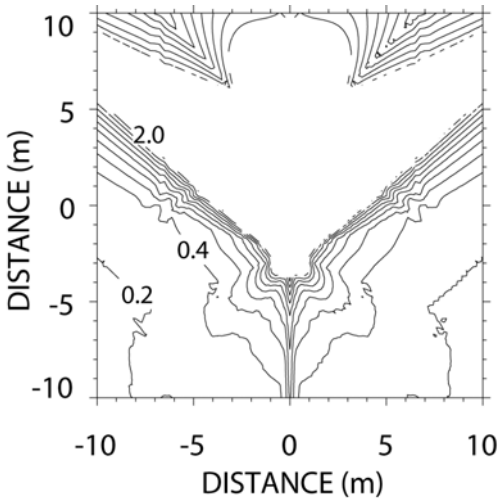

Fig 13 - The full-field predictions for b = 50 000, (f_A = 2985 Hz) (5 m column of charge)

high frequency regime it underestimates the true vibration. Nevertheless, the discrepancies are not considered prohibitive. In fact over the range 300 Hz $\leq f_A \leq$ 1000 Hz there is good agreement between both solutions, and this preserves the value of the Heelan model (especially the Scaled Heelan version) as an engineering tool for use in blast damage assessment.

DISCUSSION

Hustrulid and Wenbo (2002) have questioned the use of a pressure-time history given by the form of equation (1), and there are three pertinent points to make in this regard. Firstly, this general form was chosen because it has a long history of use in dynamic modelling (see for example, Shastri and Malumdar, 1982), with a shape similar to much experimental data (see, for example, Grady et al, 1980; Larson, 1982). Secondly, any general form (including experimental data) can be used for this pressure, $P(\tau)$, in terms of dimensionless time, τ. In this case the general wave shape, $s(\tau)$, of equation (9) is simply given by the second derivative, $\partial^2 P(\tau)/\partial\tau^2$, normalised to unity; all other parts of the recipe remain unaltered. Thirdly, the treatment of Hustrulid and Wenbo (2002) to determine a pressure-time history must be viewed with great caution. They use overly simplistic assumptions for the gas dynamics within a simplistic (although fast) dynamic code (FLAC) that, in the authors' experience, is not reliable for such analyses. In fact, the evidence for this assertion is clearly seen in their predicted pressure-time history (their Figure 6), which has unrealistic saw-tooth oscillations peaking at approximately 1.4 MPa that do not correctly resolve the short term response (< 1 ms or so). More importantly, their predicted pressures are orders of magnitude too low according to measured values, which are generally of the order GPa and not MPa (see for example, Grady et al, 1980; Larson, 1982; Nie, 1999). Furthermore, their response does not decay to zero within the blast chamber, and this, too, is incompatible with observed data. Thus any conclusions Hustrulid and Wenbo (2002) draw from their predictions of near-field vibration must be viewed with caution.

In fact the use of a pressure function given by (1) has a very distinctive advantage because, as noted earlier, the parameter b is related to the waveform frequency content. Thus far we have only altered the amplitude of elemental waveforms governed by charge weight scaling laws. However, it is also well known that the waveforms, themselves, will broaden with increasing distance from the source and this can be simply modelled by replacing b with a parameter $b(d)$, where d is the distance from each element to the monitoring point. The functional dependence of this new parameter, $b(d)$, on the distance, d, is obviously related to the seismic attenuation quality, Q, of the rock material describing its viscoelastic attenuation, however the precise functional dependence is confidential. Figure 14 shows the Scaled Heelan model for a 5 m charge column in a viscoelastic material. A direct comparison with Figure 7 shows that waveform broadening alters the radiation pattern but still predicts that the dominant energy radiates outwards, governed by the direction of initiation. One version of the full-field model of Blair (2005) has viscoelastic elements built in at the fundamental level, and the radiation patterns predicted by this model are in general agreement with those shown in Figure 14.

It was previously noted that in the near-field the Holmberg-Persson model is invalid and in the far-field it simply collapses to the charge weight scaling law. In this regard Figure 15 shows the Holmberg-Persson predictions for *vppv* (in mm/s) surrounding a 5 m column of explosive using the recommended values for K, A and B given earlier. Figure 16 shows the results for *vppv* predicted by the charge weight scaling law (8) using these same parameters but replacing w_e by the total charge weight (i.e. assuming all the explosive is concentrated at

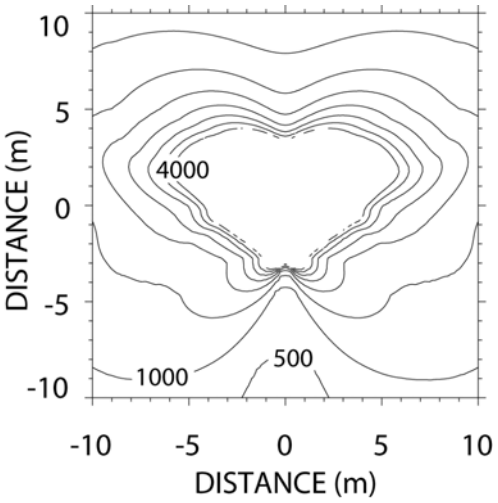

Fig 14 - The Scaled Heelan predictions for *vppv* (mm/s), 5 m charge, viscoelastic material

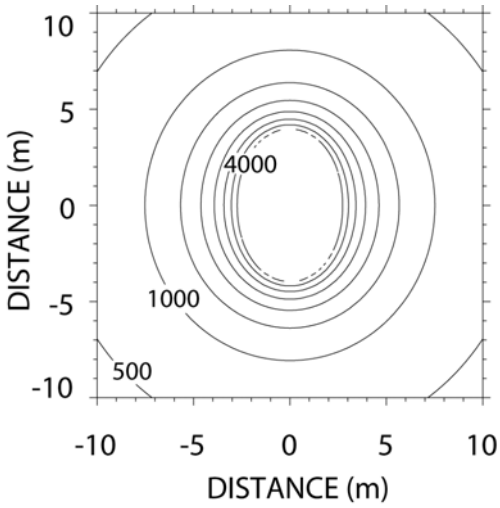

Fig 15 - The Holmberg-Persson predictions for *vppv* (mm/s) from a 5 m column of charge

the origin). It is quite clear that the simple scaling law is in good agreement with the Holmberg-Persson predictions for even moderate distances from the blasthole. In fact, if D represents any distance measure with respect to the origin (0,0) then it can be shown that the percentage difference between these two solutions is scale-independent in D/L. In this regard it should also be appreciated that these solutions depend explicitly on the total charge mass (or mass per unit length) rather than on the blasthole radius, a, itself.

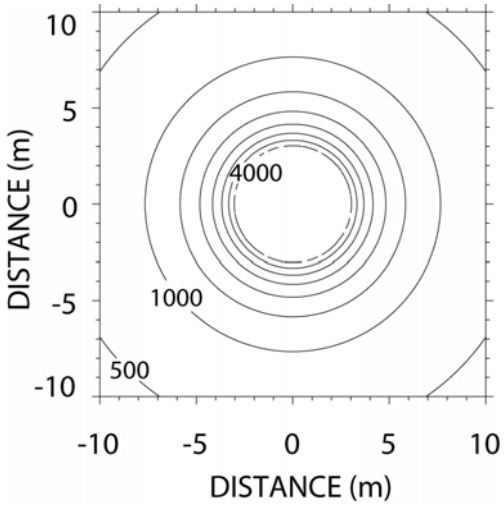

Fig 16 - The scaling law predictions for *vppv* (mm/s) from a 5 m column of charge

Figure 17 shows the percentage difference between the Holmberg-Persson model and the charge weight scaling law for dimensionless distances, D/L, surrounding a blasthole. This figure clearly shows that for horizontal distances greater than the blasthole length (i.e. $D/L > 1$) the simple scaling law is within 5 percent of the Holmberg-Persson solution. This agreement

also holds for distances greater than two blasthole lengths ($D/L > 2$) directly above (or below) the charge centre.

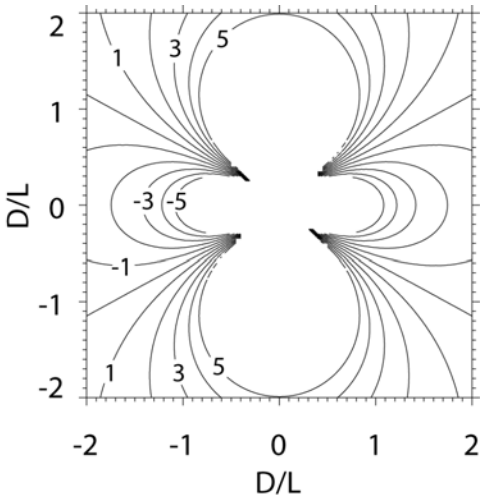

Fig 17 - Contours of percentage difference in *vppv* between the Holmberg-Persson model and a simple scaling law

Near-field vibration measurements have typical scatter much greater than 5 percent, are rarely obtained within two charge lengths of the source and even then the monitoring is only done at a scant number of locations. In this regard, the results of Figure 16 as well as the radiation patterns (see Figure 14, for example), raise two issues that are very pertinent to blast damage. Firstly, it is obvious from any practical considerations that the simple charge weight scaling law will predict peak vibration levels as well as the Holmberg-Persson model; however neither model is soundly based. Secondly, claims that the Holmberg-Persson model is a realistic predictor of experimental results are very dubious, because typical data simply do not have the required spatial coverage to determine the radiation patterns. In this regard ALL the models (including charge weight scaling as well as Holmberg-Persson) show the obvious fact that peak vibration generally decreases with decreasing charge weight and/or increasing distance from the blasthole. However, this fact alone is certainly no yardstick to determine the validity or otherwise of any particular model. In this regard, we should be guided by models that incorporate meaningful influences (such as waveform superposition, velocity of detonation etc), and show meaningful effects (such as energy transport dependent on the direction of initiation). We will then be in a position to accept (or reject) any particular waveform model whenever near-field data of sufficient quality and coverage becomes available.

CONCLUSIONS

The present work, as well as that conducted by Blair and Minchinton (1996), gives clear evidence that the Holmberg-Persson model is invalid and that there is no justification for its continued use. As an aid in this regard, we have given the detail (in recipe form) for a Scaled Heelan model that overcomes all the problems associated with the Holmberg-Persson model with the one exception of scaling dimensions. However, this exception is of little practical consequence because the Scaled Heelan model does, at least, predict numerical values of near-field vibration based on realistic waveform propagation.

In fact we have been guided, in a practical sense, by Heelan models extensively over the past ten years, and in many applications. For example, it is traditional to design blasts according to a static powder factor. However, the models clearly show that there is a preferential direction of blast effectiveness that is controlled not only by the charge weight, but also by other variables such as velocity of detonation, primer (or multiple primer) location and the relative orientation and number of blastholes. In this regard the authors have used the present Heelan techniques to

develop the concept of a dynamic powder factor for regular designs, including ring blasts for sublevel caving as reported in Minchinton and Dare-Byran (2005). As an example, Figure 18 shows the predictions of the Scaled Heelan viscoelastic model, for a standard caving ring blast. There were 11 blastholes in this design, all primed approximately 1 m above the base of the explosive column, with charge weights varying from 194 kg to 401 kg. The three central holes were initiated on the same delay, and a 25 ms delay was used between remaining groups of paired holes on either side. Only a partial extent of each hole is visible in this contour map because the remainder is obscured by the contour levels themselves.

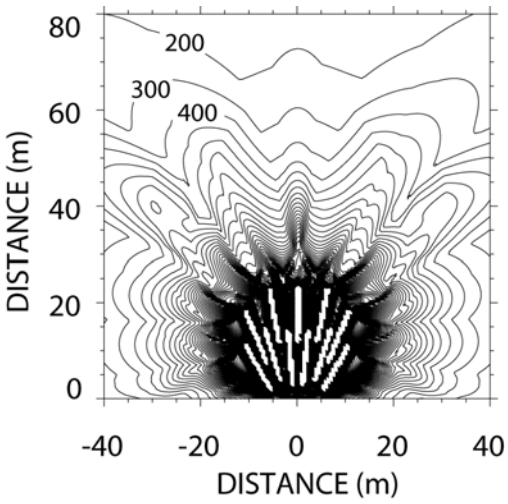

Fig 18 - Scaled Heelan predictions for *vppv* (mm/s) for a sub-level caving ring blast

REFERENCES

Adamson, W R and Scherpenisse, C R, 1998. The measurement and control of blast induced damage of final pit walls in open pit mining, in *Proceedings of 24th Annual Conference on Explosives and Blasting Techniques*, Vol II, pp 539-556, (International Society of Explosives Engineers: Cleveland).

Blair, D P, 2005. Seismic radiation from a short cylindrical charge, (Submitted).

Blair, D P, 2004. Charge weight scaling laws and the superposition of blast vibration waves, *Int J Blasting and Fragmentation*, 8(4):221-239.

Blair, D P and Minchinton, A, 1996. On the damage zone surrounding a single blasthole, in *Proceedings Fifth International Symposium on Fragmentation by Blasting - Fragblast 5,* (ed: B Mohanty), pp 121-130 (A A Balkema: Rotterdam).

Grady, D E, Kipp, M E and Smith, C S, 1980. Explosive fracture studies on oil shale, *Society of Petroleum Engineers Journal*, October:349-356.

Heelan, P A, 1953. Radiation from a cylindrical source of finite length, *Geophysics*, 18:685-696.

Holmberg, R and Persson, P A, 1979. Design of tunnel perimeter blasthole patterns to prevent rock damage, in *Tunnelling'79. Proceedings of 2nd International Symposium on Tunnelling*, (ed: M J Jones), pp 2870-283 (Institution of Mining and Metallurgy, London).

Hustrulid, W and Wenbo, L U, 2002. Some general design concepts regarding the control of blast-induced damage during rock slope excavation, in *The Seventh International Symposium on Rock Fragmentation by Blasting*, (ed: W Xuguang), pp 595-604 (Metallurgical Industry Press, Beijing).

Keller, R and Ryan, J, 2001. Considerations for the excavation of subsurface facilities by drill and blast methods, Yucca Mountain project, in *Proceedings of 27th Annual Conference on Explosives and Blasting Techniques*, Vol II, pp 39-68, (International Society of Explosives Engineers: Cleveland).

Keller, R and Kramer, N, 2000. Considerations for drill and blast excavation of a geologic repository for the disposal of high-level radioactive nuclear waste at Yucca Mountain, in *Proceedings of 26th Annual Conference on Explosives and Blasting Techniques*, Vol I, pp 31-46, (International Society of Explosives Engineers: Cleveland).

Larson, D B, 1982. Explosive energy coupling in geologic materials. *Int J Rock Mech Min Sci & Geomech Abstr,* 19:157-166.

Liu, Q, Tran, H, Counter, D and Andrieus, P, 1998. A case study of blast damage evaluation in open stope mining at Kidd Creek mines, in *Proceedings of 24th Annual Conference on Explosives and Blasting Techniques,* Vol II, pp 323-336, (International Society of Explosives Engineers: Cleveland).

McKenzie, C K, 1999. A review of the influence of gas pressure on block stability during rock blasting, in *Proceedings of Explo '99,* (ed: C Workman-Davies), pp 173-179, (The Australasian Institute of Mining and Metallurgy: Melbourne)

McKenzie, C K and Holley, K G, 2004. A study of damage profiles behind blasts, in *Proceedings of 30th Annual Conference on Explosives and Blasting Techniques,* Vol II, pp 203-226, (International Society of Explosives Engineers: Cleveland).

Meredith, J A, 1990. Numerical and analytical modelling of downhole seismic sources: the near and far field, PhD thesis, Massachusetts Institute of Technology, Boston.

Minchinton, A and Dare-Bryan, P, 2005. The application of computer modelling for blasting and flow in sublevel caving operations, in *9th AusIMM Underground Operators' Conference 2005,* pp 65-73, (The Australasian Institute of Mining and Metallurgy: Melbourne).

Nie, S, 1999. Measurement of borehole pressure history in blast holes in rock blocks, in *Proceedings Sixth International Symposium for Rock Fragmentation by Blasting,* pp 91-97, (The South African Institute of Mining and Metallurgy, Johannesburg).

Onderra, I and Esen, S, 2004. An alternative approach to determine the Holmberg-Persson constants for modelling near field peak particle velocity attenuation, *Int J Blasting and Fragmentation*, 8(2):61-84.

Onderra, I, 2004. A fragmentation modelling framework for underground ring blasting applications, *Int J Blasting and Fragmentation,* 8(3):177-200.

Ryan, J M and Harris S P, 2000. Using state of the art blast modelling software to assist the excavation of the Yucca Mountain nuclear waste repository, in *2000 High-Tech Seminar: State-of-the-Art, Blasting Technology, Instrumentation and Explosives Applications,* (ed: R F Chiappetta), pp. 407-423, (Blasting Analysis International: Allentown).

Shastri, S M and Malumdar, S, 1982. A dynamic finite element analysis of stress-wave propagation and rock fragmentation in blasting, in *Proceedings Fourth International Conference on Numerical Methods in Geomechanics*, (ed: Z Eisenstein), pp 437-447, (A A Balkema: Rotterdam).

Villaescusa, E, Onderra, I and Scott, C, 2004. Blast induced damage and dynamic behaviour of hangingwalls in bench stoping, *Int J Blasting and Fragmentation*, 8(1):23-40.